Images of Precipitation Signatures from DMSP SSM/T-2, SSM/I, and OLS

THOMAS F. LEE

Marine Meteorology Division, Naval Research Laboratory, Monterey, California

(Manuscript received 29 December 1993, in final form 13 September 13 1994)

ABSTRACT

The Special Sensor Microwave Water Vapor Sounder (SSM/T-2) is a five-channel passive microwave instrument aboard recently launched spacecraft of the Defense Meteorological Satellite Program (DMSP). Rather than address the primary purpose of the SSM/T-2, which is to retrieve atmospheric moisture, this paper examines its ability to sense precipitation as shown by images of a frontal system off the west coast of the United States. Images from the three SSM/T-2 183-GHz channels depict large regions of upper-level water vapor as evidenced by depressed brightness temperatures. Within the moist regions, even lower brightness temperatures at 183 GHz mark embedded precipitation due to volume scattering by precipitation-sized ice particles. Images of the SSM/T-2 channels at 150 and 92 GHz show ice-phase precipitation marked by low brightness temperatures and, over the ocean, low-level clouds and water vapor, both marked by warming with respect to the radiometrically cold background.

This paper compares images of precipitation from the SSM/T-2 with a coincident visible image from the DMSP Operational Line Scanner (OLS) sensor and passive microwave images from the DMSP Special Sensor Microwave/Imager (SSM/I). The discussion emphasizes potential applications to operational workstation users who are increasingly able to produce real-time SSM/T-2 images by processing direct readout telemetry. The ability to produce useful images from the 92-, 150-, and 183-GHz microwave frequencies will increase substantially when the new DMSP Special Sensor Microwave/Imager Sounder (SSM/IS) replaces the SSM/I, the SSM/T-1 (for temperature sounding), and SSM/T-2 sensors later this decade.

1. Introduction

The Defense Meteorological Satellite Program (DMSP) has installed a Special Sensor Microwave Water Vapor Sounder (SSM/T-2) aboard its F-11 satellite, which has been in orbit since November 1991. The new instrument complements the Special Sensor Microwave Temperature Sounder (SSM/T-1), which has flown on DMSP satellites since the late 1970s. The raw data from the SSM/T-1 and SSM/T-2 are processed for assimilation into numerical model analyses (Boucher et al. 1993; Nehrkorn et al. 1993). However, sensitivity of the instrument to precipitation and cloudiness in the field of view can affect the accuracy of moisture retrievals (Isaacs and Deblonde 1987; Wilheit 1990). The purpose of this paper is to exploit this sensitivity in another context by examining SSM/T-2 precipitation images. Aircraft observations and simulations show that the frequencies represented on the SSM/T-2 can give detailed depictions of precipitation (Hakkarinen and Adler 1988; Adler et al. 1990; Adler and Hakkarinen 1991). Fortunately, the spatial resolution of the SSM/T-2 sounder, though coarse compared to imaging instruments, is sufficient to create useful images. We compare images from the SSM/T-2 with images from the more established sensors aboard the DMSP satellite, including the Operational Line Scanner (OLS) visible and infrared sensor and the Special Sensor Microwave/Imager (SSM/I).

The intent of this article is to inform operational users who are increasingly able to view real-time SSM/T-2 images from processed direct readout telemetry. Although the SSM/T-2 images in this article appear at a relatively coarse spatial resolution, they foretell more detailed products to be delivered by future microwave satellite systems.

2. Instruments and data

The DMSP satellites are in a sun-synchronous, near-polar orbit at a nominal altitude of 833 km. The satellite orbital period is 102 min at an inclination of 98.8°. The DMSP SSM/T-2 is a five-channel passive microwave radiometer (Falcone et al. 1992; Griffin et al. 1993) with three channels situated symmetrically about the 183.31-GHz water vapor resonance line, a channel at 150.0 GHz, and a window channel at 91.655 GHz (Table 1). The instrument employs a cross-track scanning pattern with elongation of the field of view at the edge of scan. If unprocessed, the relatively large footprints of the SSM/T-2 produce a "jagged" appearance on the images. Thus, in this paper, a four-

Corresponding author address: Thomas F. Lee, Marine Meteorology Division, Naval Research Laboratory, 7 Grace Hopper Avenue, Monterey, CA 93943-5502.

TABLE 1. SSM/T-2 description.

Center frequency (GHz)	Nadir field of view (km)
92	84
150	54
183 ± 7	48
183 ± 3	48
183 ± 1	48

by-four bilinear interpolation is applied to create images that are smooth and easy to interpret but do not sacrifice important detail.

The DMSP SSM/I instrument (Hollinger et al. 1990) is a passive microwave radiometer operating at the frequencies of 19, 22, 37, and 85 GHz. In this paper we present images and products only from 85 GHz (field of view 15 km × 13 km) and 37 GHz (field of view 37 km × 28 km). The SSM/I senses vertically and horizontally polarized radiation at both frequencies. The instrument generates a conical scan pattern of 45° with nadir and results in a 53° angle of incidence at the surface. The SSM/I has a swath width of 1400 km, and at most latitudes there are significant gaps in coverage between successive passes. The SSM/T-2 and SSM/I swaths have considerable overlap but do not coincide completely.

3. Case study

Early on 23 March the DMSP F-11 satellite imaged a Pacific frontal cloud band moving onshore. An image of the SSM/I 85-GHz horizontal polarization (Fig. 1) shows the frontal system as a conglomeration of several indistinct features. Although it is difficult to use the 85-GHz horizontal polarization by itself to infer cloud and precipitation properties, some general conclusions are possible by inspection of the image. A band of high brightness temperatures (bright gray shades) suggests a region of high liquid water and probable rain (Petty and Katsaros 1990). An embedded region of darker gray shades suggests a convective band aloft with numerous precipitation-sized ice particles (Spencer et al. 1989). The precipitation particles scatter upwelling radiation out of the field of view of the radiometer, resulting in substantially lower brightness temperatures than surrounding regions. Bright gray shades (high brightness temperatures) result from emission from water vapor in advance of the system off the central California coast. To the rear of the system a relatively dry, cloud-free air mass allows the instrument to detect the radiometrically cold sea surface below (dark gray shades).

A polarization-corrected temperature (PCT) image (Fig. 2; Spencer et al. 1989), based on the two SSM/I 85-GHz channels, enhances the precipitation-scattering signal seen on Fig. 1. Dark gray shades on the PCT image suggest heavy precipitation along the convective band. Precipitation is faintly suggested over coastal Oregon and Washington. Like suspended ice precipitation, ground snow cover scatters energy away from the satellite, resulting in low brightness temperatures. As a result, a dark band appears on Fig. 2 over the mountainous terrain along the Canadian coast.

The technique of Katsaros et al. (1989) flags oceanic rain where SSM/I 37-GHz brightness temperatures (horizontal polarization) exceed 190 K (Fig. 3). Unlike the Spencer et al. (1989) algorithm, which exploits the scattering signature by precipitation-sized ice particles, the Katsaros et al. threshold depends on the emission from raindrops. The southern band in Fig. 3 corresponds to the convective band seen in the PCT image (Fig. 2). The northern band has no corresponding signature in the PCT image, however, suggesting little precipitation in the ice phase overlying the low-level liquid precipitation. Figure 4 combines the OLS visible image, SSM/I precipitation scattering information (Fig. 2), and SSM/I precipitation emission information (Fig. 3). Figure 4 shows that the convective band (ice above, rain below) is on the leading edge of the precipitation system with the rainband to the northwest.

Of the three SSM/T-2 183-GHz channels, the ±1 channel (imaged in Fig. 5) is weighted highest in the atmosphere and yields the lowest brightness temperatures in the moist baroclinic zone. Absorption by water vapor is sufficiently great at 183 GHz ±1 that any signature from the precipitation beneath is obscured. On the other hand, the 183 GHz ±3 and especially ±7 channels (imaged in Figs. 6 and 7) sense significantly deeper into the moist band, producing higher brightness temperatures in nonprecipitating areas than at 183 GHz ±1. In contrast, the depressed brightness temperatures caused by ice scattering delineate the embedded precipitation band well on both images. In particular, the embedded band on the 183 ± 7 image (Fig. 7) resembles the same feature on the SSM/I PCT precipitation image (Fig. 2).

Like the 183-GHz images, the image of the 150-GHz channel (Fig. 8) shows depressed brightness temperatures, due to ice particle scattering, over the embedded convective band. The radiometrically cold ocean surface, which is not sensed by any of the 183-GHz channels because of absorption by intervening water vapor, appears at 150 GHz beneath a relatively dry (and therefore relatively transparent) air mass northwest of the frontal band. The dark gray shades of the sea surface match the appearance of the convective precipitation band, complicating interpretation of the image. Brighter gray shades over the ocean indicate emission from liquid water or low-level water vapor in the frontal band.

The 92-GHz image (Fig. 9) strongly resembles the SSM/I 85-GHz image (Fig. 1). The most striking difference is the smoothed appearance of the 92-GHz image, a result of the relatively coarse SSM/T-2 resolu-

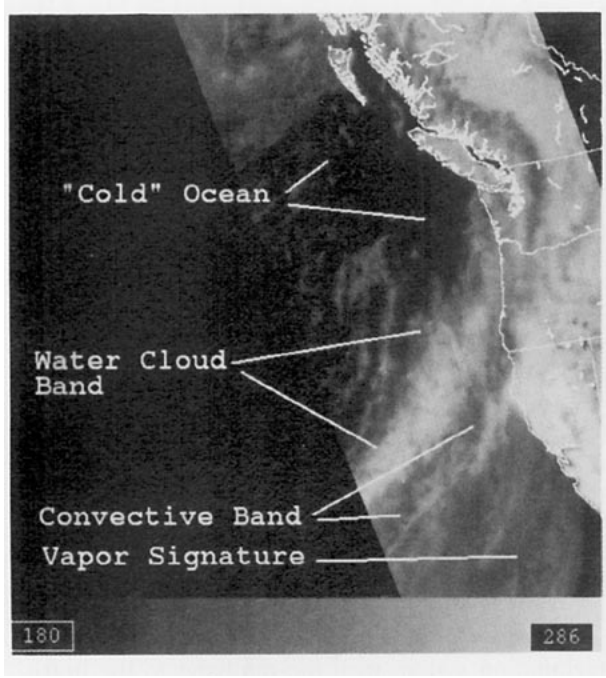

FIG. 1. DMSP SSM/I 85-GHz (horizontal polarization) image for 0109 UTC 23 March 1993. Bar at bottom gives range of brightness temperatures (K).

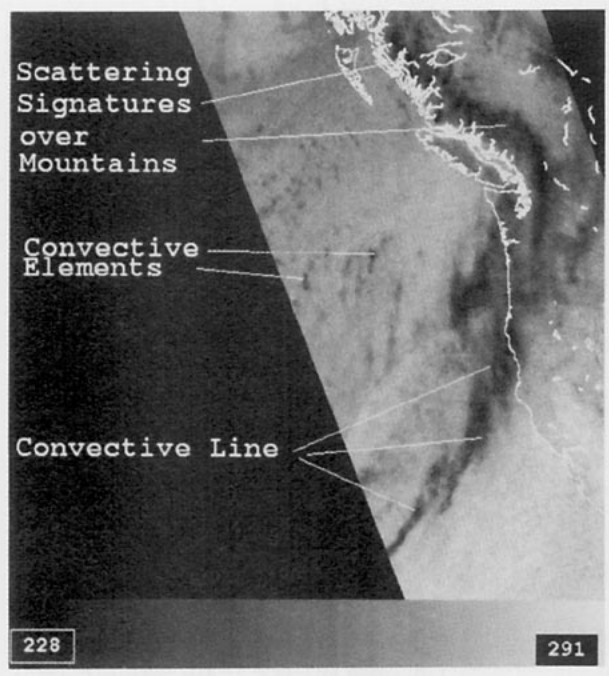

FIG. 2. DMSP SSM/I 85-GHz polarization-corrected temperature image (Spencer et al. 1989) for 0109 UTC 23 March 1993. Bar at bottom gives range of temperatures (K).

FIG. 3. DMSP SSM/I rain-flagged image based for 0109 UTC 23 March 1993. White regions over the Pacific Ocean specify 37-GHz (horizontal polarization) brightness temperatures in excess of 190 K (Katsaros et al. 1989).

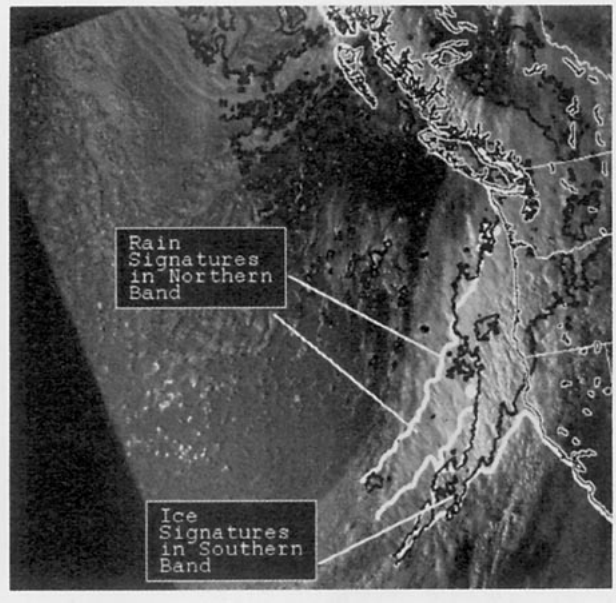

FIG. 4. DMSP visible image overlayed with an SSM/I rain flag in white contours (from information in Fig. 3) and an SSM/I precipitation scattering index in black contours (from information in Fig. 2). The threshold used for enclosure in the black contours is a scattering index less than 255 K (Spencer et al. 1989). The southern precipitation band contains significant precipitation-sized ice particles above the freezing level and rain below. The northern band contains significant rain at low levels but lacks precipitation-sized ice particles above. Disregard data over land.

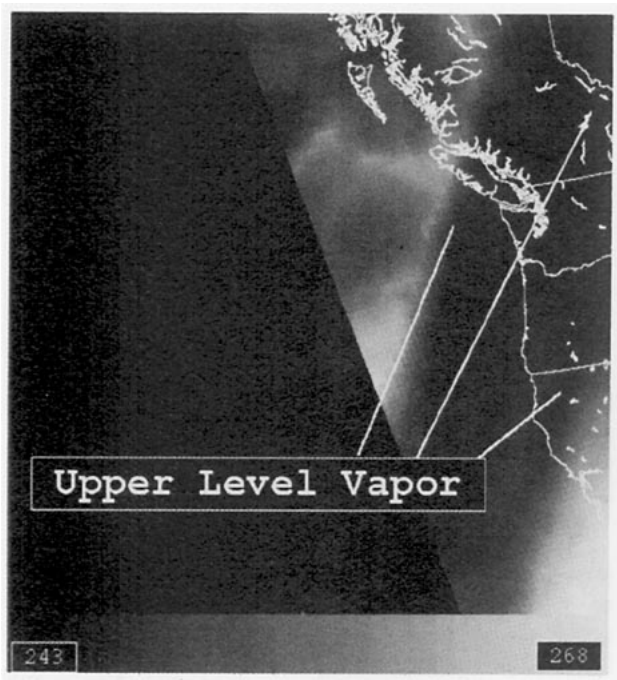

FIG. 5. DMSP SSM/T-2 183 GHz ±1.0 for 0109 UTC 23 March 1993. Bar at bottom gives range of brightness temperatures (K).

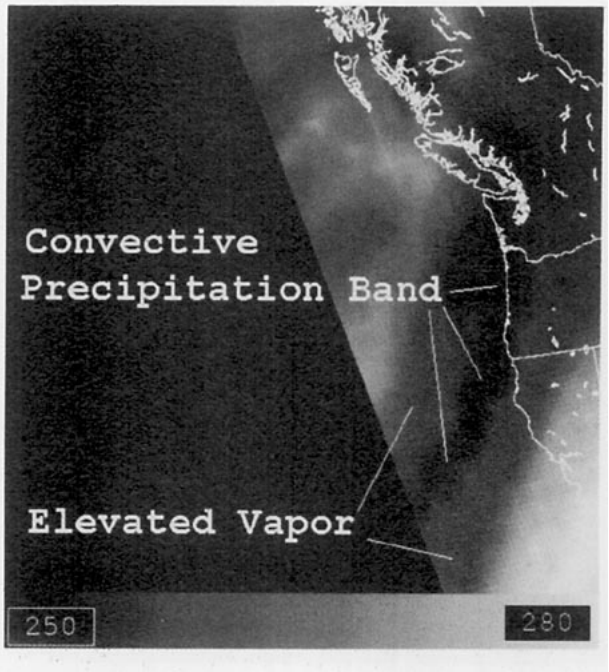

FIG. 6. DMSP SSM/T-2 183 GHz ±3.0 for 0109 UTC 23 March 1993. Bar at bottom gives range of brightness temperatures (K).

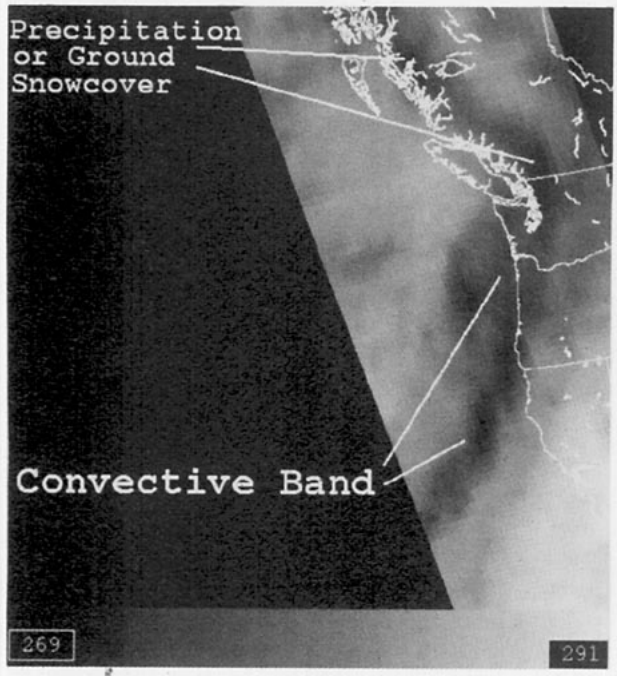

FIG. 7. DMSP SSM/T-2 183 GHz ±7.0 for 0109 UTC 23 March 1993. Bar at bottom gives range of brightness temperatures (K).

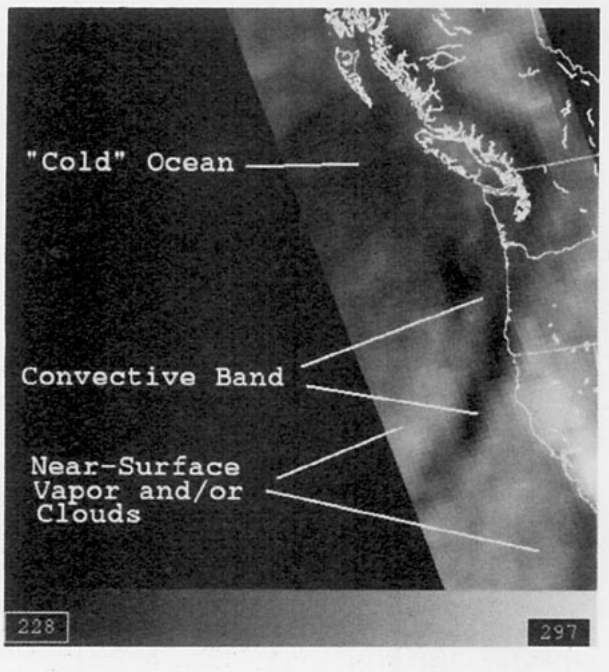

FIG. 8. DMSP SSM/T-2 150 GHz for 0109 UTC 23 March 1993. Bar at bottom gives range of brightness temperatures (K).

tion. Off the west coast of the United States, emission from rain, cloud water, and water vapor produce distinct warming (bright gray shades) with respect to the cold ocean background. An indistinct band of depressed brightness temperatures (dark gray shades), resulting from scattering by precipitation-sized particles, faintly marks the convective band observed on the previous images.

4. Discussion and conclusions

The opacity of water vapor between the satellite and the surface at 183 GHz diminishes the response to the

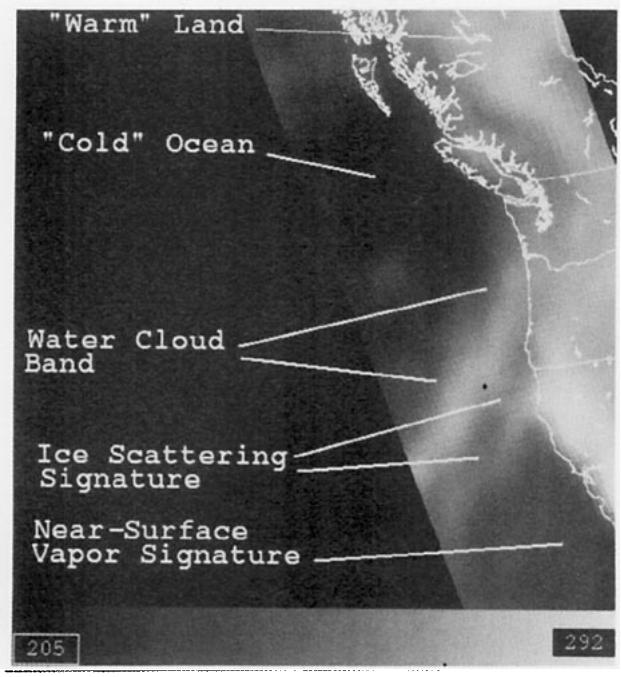

FIG. 9. DMSP SSM/T-2 92 GHz for 0109 UTC 23 March 1993. Bar at bottom gives range of brightness temperatures (K).

surface background or near-surface features. This effect, called "water vapor screening" (Gasiewski 1992), helps explain modeling results (Isaacs and Deblonde 1987) that suggest that the ±1 and the ±3 channels would be completely insensitive to water cloud, while the ±7 channels would show only minimal sensitivity. Water vapor screening explains the failure of 183-GHz images to show contrast between land and sea surfaces, contrast seen easily on images of 92 and 150 GHz.

No signatures of ice-phase precipitation are apparent in the 183-GHz ±1 (Fig. 5) image. Any such signatures are screened by strongly absorbing water vapor above the precipitation. Ice-phase precipitation signatures are apparent in images of the 183-GHz ±3 (Fig. 6) and ±7 (Fig. 7) channels, which are less subject to screening by intervening water vapor. The sensitivity of 183 GHz to precipitation above the freezing level, as opposed to low-level liquid precipitation, has been demonstrated previously with aircraft images that show superior spatial correspondence of 183-GHz images with weather radar reflectivity at 6 km than at 2 km (Hakkarinen and Adler 1988).

Images of 150 (Fig. 8) and 92 GHz (Fig. 9) show vapor, clouds, or rain against the low-emissivity ocean background, but detection against high-emissivity land backgrounds is more difficult. Ice-phase precipitation can be detected at the two frequencies over land as depressed brightness temperatures against a radiometrically warmer background. However, the depressed brightness temperatures of ice-phase precipitation are sometimes difficult to detect against a radiometrically cold ocean background or a radiometrically cold, snow-covered land surface background (e.g., Fig. 8).

DMSP products are becoming increasingly available to remote users who rely heavily on overhead satellite readout. The Naval Research Laboratory in Monterey, California, routinely receives and processes West Coast DMSP readouts on a computer workstation. Laboratory personnel intercompare images from the SSM/I, SSM/T-2, and OLS to assess how much value each could add to remote forecast efforts. Advantageously, SSM/T-2 images can show direct precipitation signatures, unlike visible and infrared images. In particular, images of the 183-GHz ±7 channel give useful depictions of ice-phase precipitation over both land and sea. However, precipitation is often shown more distinctly and with better spatial resolution by SSM/I products.

Aside from an ability to depict precipitation, SSM/T-2 images can be used as water vapor images, although interpretation is not always straightforward. For example, over oceans the appearance of water vapor depends on frequency. At 92 and 150 GHz, regions of high water vapor content are radiometrically warm (bright gray shades on images) with respect to adjacent drier regions that are radiometrically cold (dark gray shades). However, at 183 GHz the instrument does not sense deep enough into the atmosphere to detect the "cold" ocean. Thus, water vapor mass varies inversely with brightness temperature; warm temperatures represent relatively deep penetration into a dry, relatively transparent atmosphere, and cold temperatures represent shallow penetration into a moist, relatively opaque atmosphere. Thus, dark gray shades represent moist regions, and bright gray shades represent dry regions. The appearance of water vapor on 183-GHz images is similar to that on Geostationary Operational Environmental Satellite (GOES) water vapor images at 6.7 and 7.3 μm, which also weight the mid- and upper troposphere. However, GOES operational water vapor images are usually complemented, depicting moisture as bright and dry regions as dark.

The ability to image the microwave frequencies investigated here will increase substantially when the new DMSP Special Sensor Microwave/Imager Sounder (SSM/IS) replaces the SSM/I, the SSM/T-1, and SSM/T-2 sensors later in this decade (Swadley and Chandler 1991, 1992). All data will be sensed in a conical scan at a 53.1° angle of incidence with the surface of the earth. The new instrument will include 150- and 183-GHz (±1, ±3, ±7) sensing capability in the horizontal polarization. The present 85-GHz capability of the SSM/I will be replaced with a 92-GHz capability on the SSMIS with data in the horizontal and vertical polarizations. The 92-, 150-, and 183-GHz channels will all have a 12.5-km footprint size.

Acknowledgments. The support of the sponsor, the Office of Naval Research, under program element 0602435N, is gratefully acknowledged.

REFERENCES

Adler, R. F., and I. M. Hakkarinen, 1991: Aircraft multifrequency passive microwave observations of light precipitation over the ocean. *J. Atmos. Oceanic Technol.*, **8,** 201–220.

——, R. A. Mack, N. Prasad, H.-Y. M. Yeh, and I. M. Hakkarinen, 1990: Aircraft microwave observations and simulations of deep convection from 18 to 183 GHz. Part I: Observations. *J. Atmos. Oceanic Technol.*, **7,** 377–391.

Boucher, D. J., B. H. Thomas, and A. M. Kishi, 1993: Performance of the DMSP SSM/T-2 microwave radiometer: A comparison between sensor derived, model analyzed, and radiosonde measured moisture variables. Preprints, *Eighth Symp. on Meteorological Observations and Instrumentation,* Anaheim, CA, Amer. Meteor. Soc., J150–J152.

Falcone, V. J., and Coauthors, 1992: SSM/T-2 calibration and validation data analysis. Environmental Research Papers, No. 111, PL-TR-92-2293, 108 pp. [Available from Phillips Laboratory, Directorate of Geophysics, Hanscom Air Force Base, MA, 01731-5000.]

Gasiewski, A. J., 1992: Numerical sensitivity analysis of passive EHF and SMMW channels to tropospheric water vapor, clouds and precipitation. *IEEE Trans. Geosci. Remote Sens.*, **30,** 859–870.

Griffin, M. K., V. J. Falcone, J. F. Morrissey, R. G. Isaacs, J. D. Pickle, R. Kakar, J. Wang, and P. Racette, 1993: The Special Sensor Microwave Water Vapor Sounder (SSMT/T-2): Calibration study. Preprints, *Eighth Symp. on Meteorological Observations and Instrumentation,* Anaheim, CA, Amer. Meteor. Soc., J144–J149.

Hakkarinen, I. M., and R. F. Adler, 1988: Observations of precipitating convective systems at 92 and 183 GHz: Aircraft results. *Meteor. Phys.*, **38,** 164–182.

Hollinger, J. P., J. L. Pierce, and G. A. Poe, 1990: SSM/I instrument evaluation. *IEEE Trans. Geosci. Remote Sens.*, **28,** 781–790.

Isaacs, R. G., and G. Deblonde, 1987: Millimeter wave moisture sounding: The effect of clouds. *Radio Sci.*, **22,** 367–377.

Katsaros, K. B., I. Bhatti, L. A. McMurdie, and G. W. Petty, 1989: Identification of atmospheric fronts over the ocean with microwave measurements of water vapor and rain. *Wea. Forecasting,* **4,** 449–460.

Nehrkorn, T., R. N. Hoffman, J. Louis, R. G. Isaacs, and J. Moncet, 1993: Analysis and forecast improvements from simulated satellite water vapor profiles and rainfall using a global data assimilation system. *Mon. Wea. Rev.*, **121,** 2727–2739.

Petty, G. W., and K. B. Katsaros, 1990: Precipitation observed over the South China Sea by the Nimbus-7 Scanning multichannel radiometer during winter MONEX. *J. Appl. Meteor.*, **29,** 273–287.

Spencer, R. W., H. M. Goodman, and R. E. Hood, 1989: Precipitation retrieval over land and ocean with the SSM/I: Identification and characteristics of the scattering signal. *J. Atmos. Oceanic Technol.*, **6,** 254–273.

Swadley, S. D., and J. Chandler, 1991: The Defense Meteorological Satellite Program's Special Sensor Microwave Imager/Sounder (SSMIS). Preprints, *Seventh Symp. on Meteorological Observations and Instrumentation.* New Orleans, LA, Amer. Meteor. Soc., 175–178.

——, and ——, 1992: The Defense Meteorological Satellite Program's Special Sensor Microwave Imager/Sounder (SSMIS): Hardware and retrieval algorithms. Preprints, *Sixth Conf. on Satellite Meteorology and Oceanography.* Atlanta, GA, Amer. Meteor. Soc., 457–461.

Wilheit, T. T., 1990: An algorithm for retrieving water vapor profiles in clear and cloudy atmospheres from 183 GHz radiometric measurements: Simulation studies. *J. Appl. Meteor.*, **29,** 508–515.